Chemistry of Styrene (Water)$_n$ Clusters, $n = 1-5$: Spectroscopy and Structure of the Neutral Clusters, Deprotonation of Styrene Dimer Cation, and Implication to the Inhibition of Cationic Polymerization

H. Mahmoud, I. N. Germanenko, D. Wright, and M. S. El-Shall*

Department of Chemistry, Virginia Commonwealth University, Richmond, Virginia 23284-2006

Received: February 3, 2005; In Final Form: March 14, 2005

The styrene−water binary clusters SW_n, with $n = 1-5$ have been studied by the (one-color) resonant two-photon ionization technique using the 0_0^0 resonance of styrene. The structures and energetics of the neutral clusters are investigated using a search technique that employs Monte Carlo procedure. The strong tendency for water molecules to form cyclic hydrogen-bonded structures is clearly observed in the SW_n structures starting from $n = 3$. The results indicate that the spectral shifts correlate with the interaction energies between styrene and the water subcluster (W_n) within the SW_n clusters. Evidence is presented that points to (1) the formation of a covalent bonded styrene radical cation dimer following the 193 nm MPI of styrene neutral clusters, (2) proton transfer from the styrene dimer cation to the water or methanol subcluster, resulting in the formation of protonated water or methanol clusters and a styrene dimer radical, and (3) extensive solvation of the styrene dimer radical within the protonated solvent molecules. The proton-transfer reactions may explain the strong inhibition effects exerted by small concentrations of water or methanol on the cationic polymerization of styrene. These results provide a molecular level view of the inhibition mechanism exerted by protic solvents on the cationic polymerization of styrene.

I. Introduction

Styrene is the simplest molecule that contains an unsaturated group covalently linked to an aromatic ring and therefore represents a model system for studying branched aromatic rings and their interactions with polar solvents in neutral and ionized states. The unsaturated side chain can provide an additional site for the interaction with polar molecules, in competition with the aromatic ring. These interactions are relevant to a wide variety of chemical, photochemical and biological processes in many fields including polymer chemistry.[1−5] In radical and ionized systems, the reactivity of the olefin groups leads to covalent interaction resulting in the formation of styrene dimers, oligomers and polymers.

Styrene is known to undergo polymerization in bulk monomer or in solution by free radical, cationic and anionic mechanisms.[3−5] The crucial role played by the presence of trace amounts of water and other protonic impurities on the mechanism and rate of polymerization is widely recognized.[3−5] In radiation-induced polymerization of the bulk monomer, free cations are largely responsible for the polymerization under very dry conditions.[6,7] In the presence of water impurity, a slower polymerization takes place and is believed to be an entirely a free radical process.[6,7] The presence of a small amount of methanol is also known to suppress the cationic polymerization and enhances both the styrene dimerization and the radical polymerization.[8] Therefore, it is generally accepted that in radiation-induced polymerization of styrene an ionic mechanism prevails only in the dry system, whereas radical polymerization dominates in the presence of water.[3−8]

Studies of binary clusters involving styrene and water molecules can reveal the microscopic properties of aqueous solutions and their influences on the mechanism and the extent of the polymerization reactions.[9,10] Such studies are important for the elucidation of the effects of inhibitors and retarders on the efficiency of different polymerization channels such as cationic vs free radical mechanisms. The cluster environment represents an interesting medium for the study of ionic reactions in the intermediate regime between gas phase and condensed phase chemistry.[9−18] In this environment, the ionic reactions can be induced by photoionization of the styrene molecule in a binary (styrene)$_m$(water)$_n$ cluster (S_mW_n). Because of the differences in the geometry and binding energy of the neutral and the ionized cluster, the cluster ions produced ($S_m^+W_n$) are often intermolecularly vibrationally excited and can induce (initiate) ion−molecule reactions within the clusters. The ion−molecule reactions within the ionized styrene subcluster can result in the formation of covalent styrene oligomer ions. The excess energy from the exothermicity of the intracluster reactions can be dissipated by energy transfer to the low-frequency cluster modes, leading to partial evaporation of the water molecules. The evaporative cooling from clusters is analogous to collisional stabilization of the ionic intermediates in the gas phase at high pressures.[13,18] In addition, the cluster environment permits some unique cooperative effects such as those involving three-body interactions, which are generally very inefficient in the gas phase, particularly at low pressures. For example, proton transfer (PT) from the styrene oligomer radical cations to the water subcluster could lead to the termination of the ionic polymerization channel and the activation of a free radical addition reaction. The stepwise deprotonation reaction of the benzene radical cation has been recently studied in the gas phase where four water molecules were required to activate the reaction.[19] In the $S_m^+W_n$ clusters, PT from the oligomer radical cations may become more favorable than from the styrene radical cation,

* Author to whom correspondence should be addressed. E-mail: selshall@hsc.vcu.edu.

10.1021/jp050594y CCC: $30.25
Published on Web 04/28/2005

thus resulting in the formation of oligomer styrene radicals and protonated water clusters.

The objective of the present work is to study the interactions within the S_mW_n clusters in both the neutral and the radical cation states of the styrene chromophore. To distinguish between the reactions and structural features of the neutral and ionized clusters, we use resonant 2-photon ionization (R2PI) and multiphoton ionization (MPI) techniques. For the neutral clusters, we report the ultraviolet spectroscopy of the SW_n clusters with $n = 1-5$ using the 1-color R2PI technique. This study provides information on the spectral shifts imposed by water molecules in the SW_n clusters relative to the 0_0^0 origin of the isolated styrene molecule. We also investigate the structures of the SW_n clusters with $n = 1-5$, using pair-potential−Monte Carlo (MC) simulations. The combination of R2PI spectra and theoretical calculations provides a reasonably compelling picture of the interactions involved in the SW_n clusters. For the ionized clusters, we report the photodissociation products of the styrene dimer cation and investigate the effect of water on the product ions resulting from the MPI of the binary S_mW_n clusters. Finally, we discuss the implication of the current results to the inhibition mechanism exerted by water and other protic solvents on the cationic polymerization of styrene.

II. Experimental Methods

Styrene (S_m) and binary styrene/water (S_mW_n) clusters are generated by pulsed adiabatic expansion in a supersonic cluster beam apparatus.[20−23] The essential elements of the apparatus are jet and beam chambers coupled to a time-of-flight (TOF) mass spectrometer. The clusters are formed in a He-seeded jet expansion, and probed as a skimmed cluster beam in a collision-free high vacuum chamber with a delay between synthesis and probe (i.e., the neutral beam flight time) on the order of 1 ms. During operation, a vapor mixture of styrene−water is prepared by flowing He (ultrahigh purity, Spectra Gases 99.999%) over the two separate temperature-controlled liquids and mixing these flows with the main flow of He. The vapor mixture at a pressure of 8 atm is expanded through a conical nozzle (100 μm diameter) in pulses of 200−300 μs duration at repetition rates of 10−15 Hz. The jet is skimmed and passed into a high vacuum chamber, which is maintained at 8×10^{-8} to 2×10^{-7} Torr. The collimated cluster beam passes into the ionization region of the TOF mass spectrometer where it intersects a laser pulse from a frequency-doubled dye laser. The tunable radiation is provided by a dye laser (Lambda Physik FL3002) pumped by an excimer laser (Lambda Physik LPX-101). Coumarin 540A (Exciton) dye laser output passes through a β-BaB_2O_4 crystal to generate a continuously tunable frequency-doubled output of 10^{-8} s pulses. The spatially filtered (using a set of four quartz Pellin-Broca prisms) ultraviolet radiation is adjusted to minimize three photon processes while still providing sufficient ion current (photon power density $\approx 2.5 \times 10^5$ W/cm^2). The cluster ions formed by the R2PI are electrostatically accelerated in a two-stage acceleration region (300−400 V/cm) perpendicular to the direction of the neutral beam and then travel a field-free region (170 cm in length) to a two-stage microchannel-plate detector. Deflection plates are used to compensate for the ion beam velocity in the direction of the neutral cluster beam. The TOF spectrum is recorded by digitizing the amplified current output of the detector with a 500 MHz digitizer (LeCroy 9350A) and averaged over 200 pulses. In the MPI experiments, the clusters are ionized by laser pulses from an excimer laser (Lambda Physik) using the KrF (248 nm) or the ArF (193 nm) line.

The R2PI spectra presented in the paper were selected from a great number of experiments under a range of conditions, characterized primarily by the concentrations of styrene and water vapors in the preexpansion mixture, the seed ratio in He and total pressure. The relative concentrations studied (styrene:water:He) ranged from $(1:(1 \times 10^2):(5 \times 10^7))$ to $(1:(6 \times 10^2):(6 \times 10^7))$. Several concentration studies were performed to identify the spectral features arising from different cluster series such as the S_2W_n and S_3W_n series. The reported spectra were all obtained with the minimum concentration of styrene vapor in the preexpansion mixture that allowed the observation of mainly the SW_n series (the lowest concentration of styrene corresponded to a sample temperature of −75 °C at which the vapor pressure is roughly 2×10^{-4} Torr). We have performed repeated sets of experiments with different concentrations of water in the preexpansion series to control the distribution of the SW_n neutral clusters. For example, the spectra of the SW and SW_2 clusters were confirmed by using trace concentration of water vapor (by flowing He over water kept at −65 °C corresponding to a vapor pressure of 6.7×10^{-3} Torr). The spectral features that showed dependence on the water concentration in the preexpansion mixtures were confirmed to be arising from higher clusters. All the spectral features reported in the paper were reproduced many times under a variety of concentration and laser power conditions.

III. Computational Methods

Cluster interaction energies were calculated from site−site potentials of the form

$$\Delta e_{ab} = \sum_i^{ona} \sum_j^{onb} \left(\frac{q_i q_j e^2}{r_{ij}} + \frac{A_{ij}}{r_{ij}^{12}} - \frac{C_{ij}}{r_{ij}^{6}} \right) \quad (1)$$

where Δe_{ab} is the interaction energy between two molecules a and b, the A_{ij} and C_{ij} can be expressed in terms of the Lennard-Jones σ's and ϵ's as $A_{ii} = 4\epsilon_i\sigma_i^{12}$ and $C_{ii} = 4\epsilon_i\sigma_i$,[6] and the combining rules $A_{ij} = (A_{ii}\,A_{jj})^{1/2}$ and $C_{ij} = (C_{ii}C_{jj})^{1/2}$ were used. The q_i are the partial charges assigned to each site and e is the magnitude of the electron charge.

For water, the 4-site OPLS/TIP4P potential was used.[24] For the sites (O, H, M) (M is the negatively charged site 0.15 Å from the O) the σ's are (3.154, 0, 0), the ϵ's are (0.155, 0, 0), and the q's are (0, 0.52, −1.04). The H−O bond length is 0.9572 Å and the HOH angle is 104.52°. For styrene, a 16-site (all-atom) model was developed that includes the internal rotation of the ethylene group, as described in ref 25.

The total cluster configurational energy can be expressed as

$$\Delta E = \Delta E_{\mathrm{C}} + \Delta E_{\mathrm{LJ}} + \Delta E_{\mathrm{S}} \quad (2)$$

where ΔE_{C} is the sum of all terms representing Coulomb interactions, ΔE_{LJ} the sum of all Lennard-Jones terms, and ΔE_{S} the intramolecular torsional energy of the styrene. Alternatively, the total energy can be expressed as

$$\Delta E = \Delta E_{\mathrm{W}} + \Delta E_{\mathrm{S-W}} + \Delta E_{\mathrm{S}} \quad (3)$$

where ΔE_{W} is the sum of all terms involving water−water interactions and $\Delta E_{\mathrm{S-W}}$ is the sum of all terms involving styrene−water interactions.

The software used for the Monte Carlo simulations was developed in our laboratory and has been used in several previous studies.[21,25−27] Many of the core routines were adapted from Jorgensen's MCLIQ (1990) program.[28]

Cluster structures and energies are obtained through the following simulation procedure. Monte Carlo simulations in the

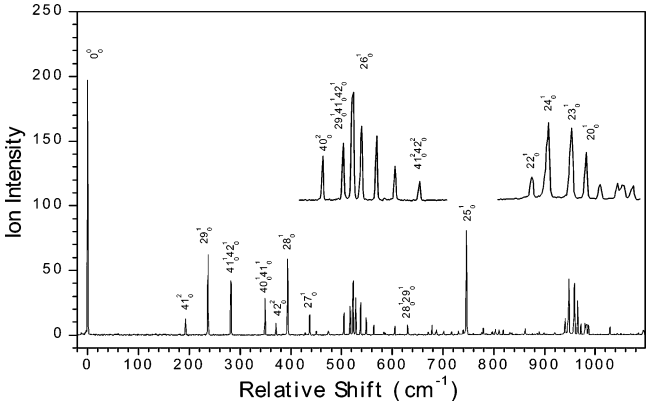

Figure 1. One-color R2PI spectra measured in the styrene (S) mass channel relative to the electronic origin band of the $S_1 \leftarrow S_0$ transition of the styrene molecule at 34 758.79 cm^{-1}.

NVT ensemble are run for each cluster size using standard procedures, without truncation of the potential and at a temperature at which no evaporation is observed. At regular intervals during these simulations, the current cluster configuration is taken as an initial structure for a "quench" in which the cluster is settled into the underlying minimum on the potential surface. This is done by accepting only those small random displacements and rotations that lower the potential energy. Eventually, a minimum is reached, and when 6000 consecutive trial configurations fail to find a structure of lower energy, the configuration is identified as a candidate for a minimum on the surface. Subsequently, in a separate calculation, each candidate is run at 10^{-12} K to confirm that a minimum has in fact been found and to be sure that the bottom of the well has been reached. For each cluster composition C_8H_8-$(H_2O)_n$, 1000−1500 quenches were performed except for $n = 1$, where only 500 were done. Most minima were located numerous times.

IV. Results and Discussion

IV-1. R2PI Spectra of Styrene (Water)$_n$ Clusters, $n = 1-5$. The electronic origin band of the $S_1 \leftarrow S_0$ transition of styrene is located at 34 758.79 cm^{-1} (287.697 nm) and the transition moment is parallel to the long in-plane axis.[29−32] Figure 1 displays the R2PI spectrum obtained by monitoring the mass channel corresponding to styrene (S) in the 0_0^0 region between 34 700 and 35 700 cm^{-1}. The spectrum shows the 0_0^0 origin and several vibronic bands as well as cross-sequence bands, and the overall spectrum is in very good agreement with previous fluorescence excitation and REMPI studies.[31,33,34]

The R2PI mass spectrum obtained at 287.165 nm is shown in Figure 2. In addition to the major clusters' series SW_n, the mass spectrum shows the relatively strong styrene dimer (S_2) as well as the S_2W_n series.

Figure 3 presents the R2PI spectra obtained by monitoring the mass channels corresponding to SW_n with $n = 1-5$, in the 0_0^0 region of the styrene monomer between 34 700 and 34 900 cm^{-1}. In all the spectra displayed in Figure 3, the cluster origin peak is marked with (∗) and the peaks corresponding to the van der Waals (vdW) intermolecular vibrations of the clusters are labeled with (●).

The SW mass channel shows several strong features identical to the features that appear in the SW_2 channel. These features are assigned to the SW_2 cluster with a sharp origin peak blue shifted relative to the 0_0^0 transition of the styrene by 45.7 cm^{-1}. In addition, a weak peak at 21.5 cm^{-1} is assigned to the origin

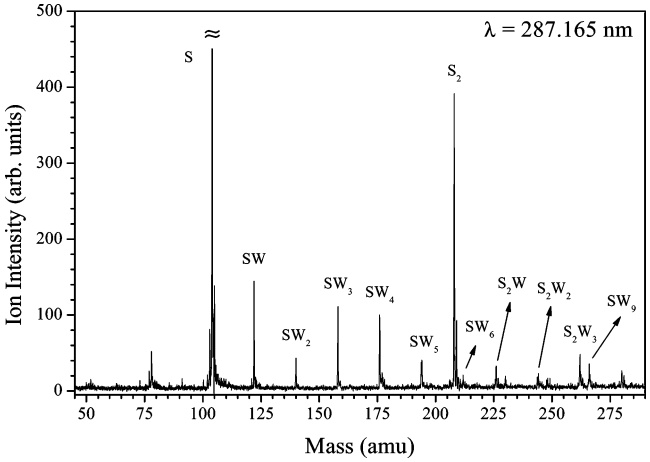

Figure 2. R2PI mass spectrum of the styrene−water (SW_n) cluster beam obtained at the resonance ionizations assigned to the origin of SW_3 cluster (287.165 nm). The unlabeled peaks at $m/z = 78$, 230, 248, and 280 are assigned to the $C_6H_6^+$ fragment from the styrene ion, SW_7, SW_8 and S_2W_4, respectively. The peaks at 1 amu below and above the styrene parent peaks (S and S_2) are assigned to hydrogen loss (C_8H_7) and ^{13}C contributions, respectively. Note that the S peak (m/z 104) is saturated (off scale).

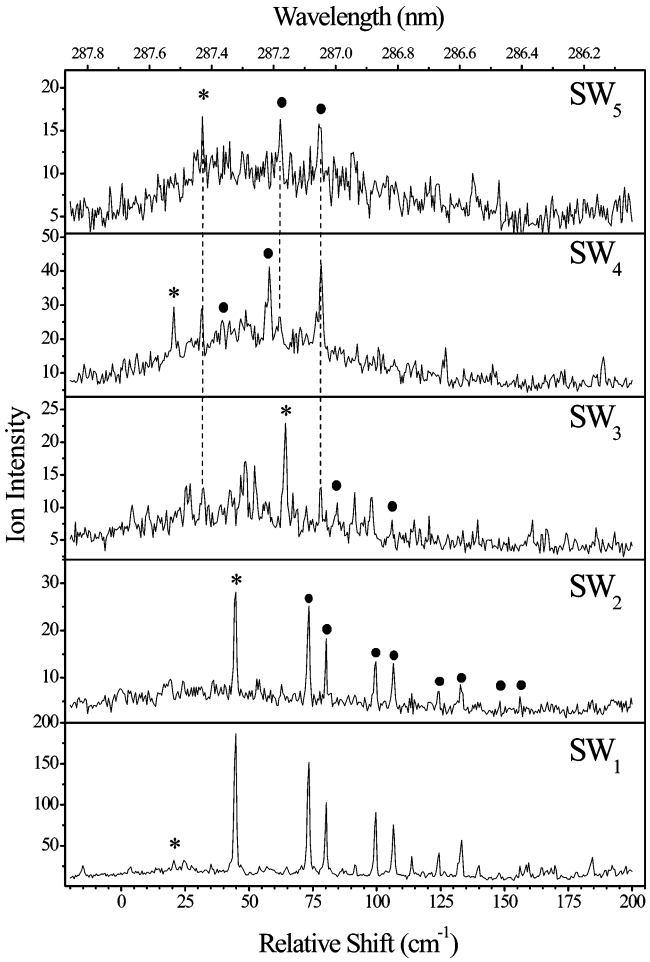

Figure 3. Overall R2PI spectra measured in the styrene (water)$_n$ mass channels (SW_n) with $n = 5$, relative to the electronic origin band of the $S_1 \leftarrow S_0$ transition of the styrene molecule at 34 758.79 cm^{-1}.

of the SW complex. Two other small peaks at 25 and 35 cm^{-1} are assigned to low-frequency vdW vibrations of the SW complex.

A rich spectrum is observed in the SW_2 mass channel with all the features appearing in the SW channel as a result of

efficient loss of a water molecule from the SW_2 cluster upon photoionization. The origin of the SW_2 cluster possesses two vdW progressions: the first appears as the set of peaks at 73, 100, 125 and 148 cm^{-1} and the second progression corresponds to peaks at 80, 107, 133 and 156 cm^{-1}, as shown in the SW_2 channel in Figure 3. The very rich intermolecular Franck−Condon activity of the SW_2 cluster indicates a large change in the geometry of the cluster following the electronic excitation of the cluster. The assignments of the origins of the SW and SW_2 clusters were supported by studying the spectral dependence on the water vapor concentration in the preexpansion mixture.[35] The results indicated that the peak at 45.7 cm^{-1} (assigned to the SW_2 origin) decreases much more rapidly with decreasing water concentration as compared to the peak at 21.5 cm^{-1} (assigned to the SW origin). This behavior suggests that the two peaks must represent different water containing clusters.[35]

The most prominent features in the SW_3 mass channel can be assigned to the origin of the SW_3 cluster at 64 cm^{-1}. Two peaks at 84.7 and 106.1 cm^{-1} relative to the 0_0^0 of styrene are assigned the vdW progressions developed on the SW_3 origin. There are several other features present in the R2PI scan of the SW_3 mass channel such as the peaks at 31.8 and 77.3 cm^{-1} that appear to be coming from the fragmentation of the SW_5 cluster. The remaining features in the SW_3 mass channel are not assigned.

The blue shifts observed for the SW_n clusters with $n = 1-3$ (21.2, 44.8 and 64.2 cm^{-1}, respectively) are consistent with weak hydrogen-bonding interactions between water and the styrene π-system. This is exactly the same trend found in the styrene (methanol)$_n$, SM_n, clusters, where the observed shifts were 63.4, 83.8 and 181.6 cm^{-1} for $n = 1$, 2 and 3, respectively. However, in the SW_n clusters the increase in the blue shift with the number of water molecules in the cluster appears to be more regular. This may suggest that the structure of the SW_3 cluster could involve two water molecules on one side of styrene and the third water on the other side of styrene (1 + 2 structure).

The blue spectral shift decreases for the origin band of the SW_4 cluster at 20.7 cm^{-1} as shown in the SW_4 mass channel in Figure 3. This observation suggests that the bonding in the SW_4 cluster may involve significant dispersion interactions between the styrene molecule and the water tetramer subcluster. The relatively strong bonding in the SW_4^+ cluster ion is also reflected in the low fragmentation probability of SW_4^+ ion as discussed below. Two vdW bands are assigned to the SW_4 cluster at 39.7 and 58.1 cm^{-1} relative to the 0_0^0 band of the styrene molecule. The other spectral features at 31.8, 62.3 and 77.3 cm^{-1} in the SW_4 mass channel are assigned to the SW_5 cluster.

In the SW_5 mass channel, three major spectral features are assigned to the SW_5 cluster. The 0_0^0 origin band of the SW_5 cluster is blue shifted by 31.8 cm^{-1} relative to the styrene's origin as shown in Figure 3. The built-in progression of vdW modes is located at 62.3 and 77.3 cm^{-1}. The SW_5^+ cluster ion experiences considerable fragmentations into the SW_4 and SW_3 mass channels as shown in Figure 3. The tentative assignments of the R2PI spectra of the SW_n clusters with $n = 1-5$ are given in Table 1.

The assignments of the SW_n origins are complicated by the efficient fragmentation of the ionized clusters as a direct result of the structural change between the neutral and the ionized cluster. The ionization potential of the styrene molecule is 68 267 cm^{-1}.[36] Because the 0_0^0 transition is located at 34 758.79 cm^{-1}, two photons resonant with the origin transition suffice to ionize styrene in a one-color REMPI experiments. The additional energy imparted to the S^+W_n cluster ion promotes fragmentation via solvent evaporation from the cluster. If the time scales for the post-ionization fragmentation processes [$S^+W_n \rightarrow S^+W_{n-m}$] are faster than the time of acceleration in the mass spectrometer, then the resonant intensity of cluster n will contribute to the observed intensity of cluster $n-m$. These time scales will in general depend on the cluster's internal energy prior to excitation, the final energy state produced by ionization, and the time scale of energy relaxation into the intermolecular modes.

TABLE 1: Spectral Features Observed in the SW_n Mass Channels (S = Styrene, W = Water, vdW = van der Waals Mode)

cluster	shift (cm^{-1}) from the 0_0^0 of styrene	obsd mass channel	rel intens	assignments	shift (cm^{-1}) from cluster's origin
SW	21.2	SW	30.4	SW origin	0
SW_2	44.8	SW	285.7	SW_2 origin	0
	44.8	SW_2	40.3	SW_2 origin	0
	73.4	SW	220.8	vdW	28.6
	73.4	SW_2	30.7	vdW	28.6
	99.6	SW	171.3	vdW	54.8
	99.6	SW_2	23.7	vdW	54.8
	106.7	SW	149.8	vdW	61.9
	106.7	SW_2	18.8	vdW	61.9
	124.3	SW	103.5	vdW	79.5
	124.3	SW_2	15.4	vdW	79.5
	133.1	SW	155.5	vdW	88.3
	133.1	SW_2	18.0	vdW	88.3
	148.1	SW	43.3	vdW	103.3
	147.6	SW_2	7.8	vdW	102.8
	156.2	SW	49.8	vdW	111.4
	156.0	SW_2	7.6	vdW	111.2
SW_3	64.2	SW_3	22.6	SW_3 origin	0
	84.7	SW_3	107	vdW	20.5
	106.1	SW_3	8.0	vdW	41.9
SW_4	20.7	SW_4	29.4	SW_4 origin	0
	39.7	SW_4	25.6	vdW	19.0
	58.1	SW_4	41.3	vdW	37.4
SW_5	31.8	SW_3	12.8	SW_5 origin	0
	31.8	SW_4	29.1	SW_5 origin	0
	31.8	SW_5	16.6	SW_5 origin	0
	62.3	SW_4	26.4	vdW	30.5
	62.3	SW_5	16.3	vdW	30.5
	77.3	SW_3	13.1	vdW	45.5
	77.3	SW_4	42.2	vdW	45.5
	77.3	SW_5	15.8	vdW	45.5

Fragmentation probabilities are measured by comparing the absolute integrated intensities I_n at various mass channels (parent I_n and daughters I_{n-1}, I_{n-2}, etc.) at the laser wavelength of a specific spectral resonance and normalizing to the sum over $I_n + I_{n-1} + ...$ etc. The results expressed as a percent of the parent ion intensity are shown in Table 2.

Within the two photon's energy limit, 93% of the SW complex fragments into the styrene mass channel upon photoionization. The fragmentation efficiency of the $SW_2^+ \rightarrow SW^+$ process is estimated as 63% from the origin peak. The SW_2^+ cluster ion also fragments into the S^+ mass channel by the loss of two water molecules (29% at the SW_2 origin at 45.7 cm^{-1}). The fragmentation efficiency decreases in the larger clusters (39% and 20% for the $SW_3^+ \rightarrow SW_2^+$ and $SW_4^+ \rightarrow SW_3^+$ processes, respectively). However, the SW_5^+ exhibits significant fragmentation (44%) to the SW_4^+ and even to the SW_3^+ channels. These observations are related to the structures and stabilities of both the neutral and the ionized clusters. For example, the very efficient fragmentation observed for the S^+W and S^+W_2 clusters following photoionization is a direct consequence of the π-hydrogen-bonded geometry of the neutral

TABLE 2: Fragmentations Probabilities of the SW_n Cluster Ions

fragmentation channel	parent, shift (cm^{-1})	%
$SW^+ \rightarrow S^+$	SW origin (21.2)	93.2
$SW_2^+ \rightarrow SW^+$	SW_2 origin (44.8)	62.6
	vdW 1 (73.4)	67.5
	vdW 2 (80.2)	67.7
	vdW 3 (99.6)	66.5
	vdW 4 (106.6)	63.0
$SW_2^+ \rightarrow S^+$	SW_2 origin (44.8)	29.3
	vdW 1 (73.4)	21.6
	vdW 2 (80.2)	21.6
	vdW 3 (99.6)	24.6
	vdW 4 (106.6)	24.6
$SW_3^+ \rightarrow SW_2^+$	SW_3 origin (64.7)	39.3
$SW_4^+ \rightarrow SW_3^+$	SW_4 origin (20.7)	19.6
$SW_5^+ \rightarrow SW_4^+$	SW_5 origin (31.8)	43.9

TABLE 3[a]

$n(I)$	$-E_n$	$-E_n/n$	$-E_n^C$	$-E_n^C/n$	$-E_{H_2O}$	$-E_{C_8H8}$	$-E_{C_8H8\rightarrow H_2O}$
1	4.03	2.01	3.59	1.79	0.00	−0.01	4.03
2(a)	11.58	3.86	12.56	4.19	6.09 (6.24)	−0.05	5.51
2(b)	11.12	3.71	11.95	3.98	5.10	−0.06	6.05
3(a)	22.34	5.59	26.24	6.56	15.74 (16.74)	−0.05	6.63
3(b)	15.32	3.83	15.72	3.93	5.89	−0.16	9.51
4(a)	33.73	6.75	40.38	8.08	26.97 (27.88)	−0.03	6.77
4(b)	33.69	6.74	39.90	7.98	26.31	−0.05	7.41
5(a)	42.65	7.11	50.66	8.44	35.09 (36.37)	−0.03	7.58
5(b)	41.16	6.86	50.16	8.36	33.67	0.00	7.49

[a] I is the isomer number (a) or (b), and n is the number of water molecules in the cluster. E_n is the total cluster configurational energy, E_n^C is the Coulomb contribution to E_n, E_{H_2O} is the energy of the water subcluster, $E_{C_8H_8}$ is the torsional energy of the styrene, and $E_{C_8H_8\rightarrow H_2O}$ is the interaction energy between the styrene and the water subcluster. The values in parentheses in the E_{H_2O} column are the water energies when the styrene is removed and the water subcluster is allowed to relax to the nearest minimum. Energies are in kcal/mol.

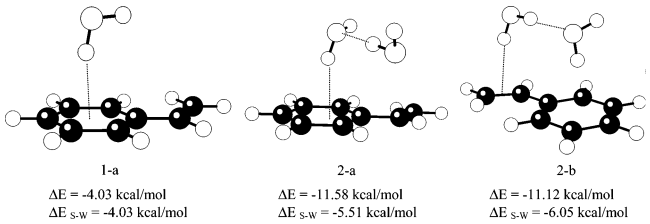

Figure 4. (1-a) Lowest energy structure of styrene (water) cluster. (2-a) Lowest energy structure of styrene $(water)_2$ cluster. (2-b) Styrene $(water)_2$ isomer with the largest styrene−$(water)_2$ interaction.

complex. The structural change in going from the π-hydrogen-bonding geometry in the neutral species to the predominantly ion−dipole interaction in the ionized species involves a great strain, which leads to efficient fragmentation.

IV-2. Structures and Energies of Styrene $(Water)_n$ Clusters, $n = 1-5$. The interaction energies of the most stable isomers of SW_n clusters and the isomers exhibiting the strongest styrene ⇔ $(water)_n$ interactions (ΔE_{S-W}) are summarized in Table 3, and the corresponding structures are displayed in Figures 4−7.

For $n = 1$, all 500 quenches gave the same cluster energy, presumably the same isomer. This structure places the water above the phenyl ring of styrene with the hydrogen of the OH group pointing toward the center of the ring as shown in Figure 4-(1-a). This is a direct result of the columbic attraction between H and the π-system. The structure is similar to that of the benzene (water) cluster obtained by Jorgensen and Severance[28] and also similar to the styrene (methanol) structure determined in our previous study.[25]

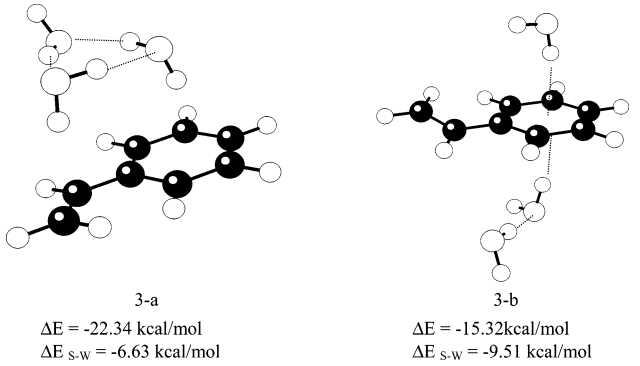

Figure 5. (3-a) Lowest energy structure of styrene $(water)_3$ cluster. (3-b) Styrene $(water)_3$ isomer with the largest styrene−$(water)_3$ interaction.

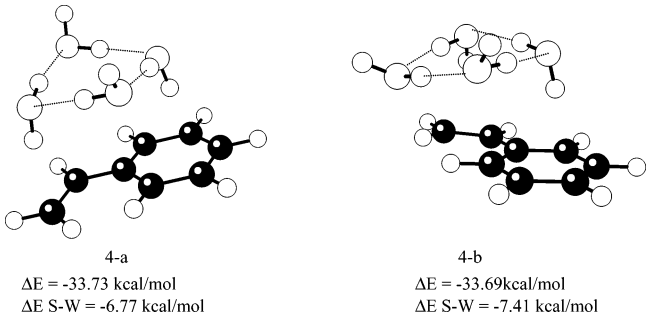

Figure 6. (4-a) Lowest energy structure of styrene $(water)_4$ cluster. (4-b) Styrene $(water)_4$ isomer with the largest styrene−$(water)_4$ interaction.

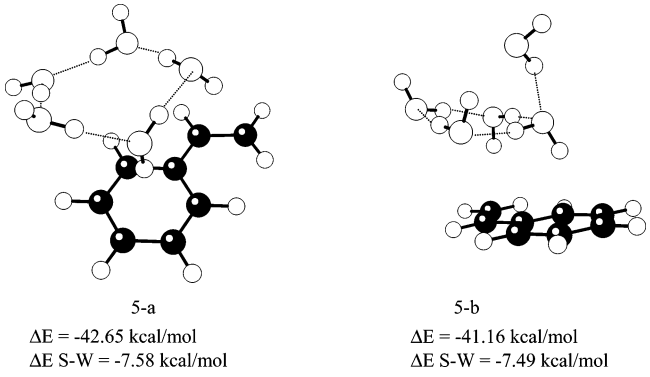

Figure 7. (5-a) Lowest energy structure of styrene $(water)_5$ cluster. (5-b) Styrene $(water)_5$ isomer with the largest styrene−$(water)_5$ interaction.

For $n = 2$, 1487 of the 1500 quenches gave structure (2-a) in Figure 4 as the lowest energy structure with the remaining 13 quenches finding seven additional structures, for a total of eight isomers. In all cases both water molecules are found in the same side of the styrene. In isomer (2-b), the water dimer has the strongest interaction with the styrene molecule through two H-bondings to the phenyl ring and the olefin group. The difference in the binding energies between structures (2-a) and (2-b) is only 0.5 kcal/mol. However, in isomer (2-b) the interaction energy of the isolated water dimer is more perturbed by the presence of the styrene than in isomer (2-a), as shown by the values in parentheses in Table 3.

For $n = 3$, a total of six isomers were located with the lowest energy isomer (3-a), displayed in Figure 5, being the only isomer having a cyclic water structure and the only isomer having all three water molecules on the same side of the styrene. All other structures show a water dimer on one side of the styrene, and a single water molecule on the other side. This is bit surprising,

yet these "2+1" structures give stronger overall water binding to the styrene as in isomer (3-b), shown in Figure 5, which exhibits the stongest ΔE_{S-W} interaction. This indicates that the interactions of styrene with the water dimer on one side and a single water molecule on the other side of the styrene ring provide extra ΔE_{S-W} interaction over the interaction resulting from the cyclization of the water trimer above the styrene molecule. This is clearly due to the H-bonding interactions between water molecules and the styrene ring. However, the overall stability of the SW_3 cluster is maximized through the incorporation of a cyclic water trimer. In this structure the interaction energy of the isolated cyclic water trimer is little perturbed by the presence of the styrene, as shown by the values in parentheses in Table 3.

For $n = 4$, six isomers of lowest energy were located, and all five lowest energy structures show a cyclic water tetramer on one side of the styrene molecule. The lowest energy and the strongest ΔE_{S-W} interaction isomers (4-a and 4-b, respectively) are shown in Figure 6. In isomer 4-a the water tetramer is pretty much on top of the styrene, whereas in isomer 4-b it is off to the side. In both isomers, the interaction energy of the water subcluster is little perturbed by the presence of the styrene, as shown by the values in parentheses in Table 3.

For $n = 5$, the 1000 quenches identified more than 50 candidates for isomers. In the six lowest energy isomers, all five water molecules are arranged in a cyclic pentamer (or "4+1") structure on the same side of the styrene as shown in the lowest energy and the strongest ΔE_{S-W} interaction isomers (5-a) and (5-b), respectively, shown in Figure 7. Again, in isomer (5-a) the interaction energy in the isolated water pentamer is not strongly affected by the presence of the styrene.

IV-3. Correlation with Observed Spectral Shifts. The spectral shifts reflect the difference in the cluster's binding energies in the ground and excited states, which are determined by the nature of the intermolecular interactions between styrene and water molecules. A red shift implies that the excited state is more tightly bound than the ground state, and a blue shift is associated with stronger interaction in the ground state. A red shift is usually observed in clusters where the dispersion energy is dominant due to the increase in the molecular polarizability in the excited state relative to the ground state.[37] For example, ring−ring interactions result in red shifts because dispersive forces are stronger for the more delocalized excited states, as in benzene and other aromatic clusters.[38] On the other hand, hydrogen-bonding to the π-system results in a blue shift, which tends to increase with increasing the H-bond donating capacity of the solvent molecules.[39]

Figure 8-a presents the observed spectral shifts of the SW_n cluster origins, with respect to the 0_0^0 band of the styrene molecule, as a function of the number of water molecules. The first three clusters of SW_n ($n = 1-3$) exhibit linear increases in the direction of spectral blue shift, with a maximum of 64.2 cm^{-1} for the SW_3 cluster. These shifts are consistent with H-bonding to the π-system of styrene. The spectral shift reverses direction in the single isomer observed for the SW_4 cluster. The successive addition of water molecules to the SW complex leads to a stable cyclic water tetramer in SW_4 that is unable to H-bond to the styrene π-system, consistent with the observed red shift. The observed pattern reveals an interesting correlation with the calculated structures of the clusters shown in Figures 4−7. Figure 8-b shows good correlations between the observed relative shifts from experiment and the calculated styrene−water subcluster interaction energies when one uses the isomer having the greatest styrene−water interaction (ΔE_{S-W}) at each cluster size, or if one averages over all lowest energy isomers located. On the other hand, if the lowest-total energy isomer is taken at each cluster size, the correlation is lost. Because the calculated ΔE_{S-W} pertains to the cluster ground state, the strong correlation between styrene-to-water interaction and spectral shift suggests that these shifts are mainly dependent on the ground-state styrene-to-water interaction.

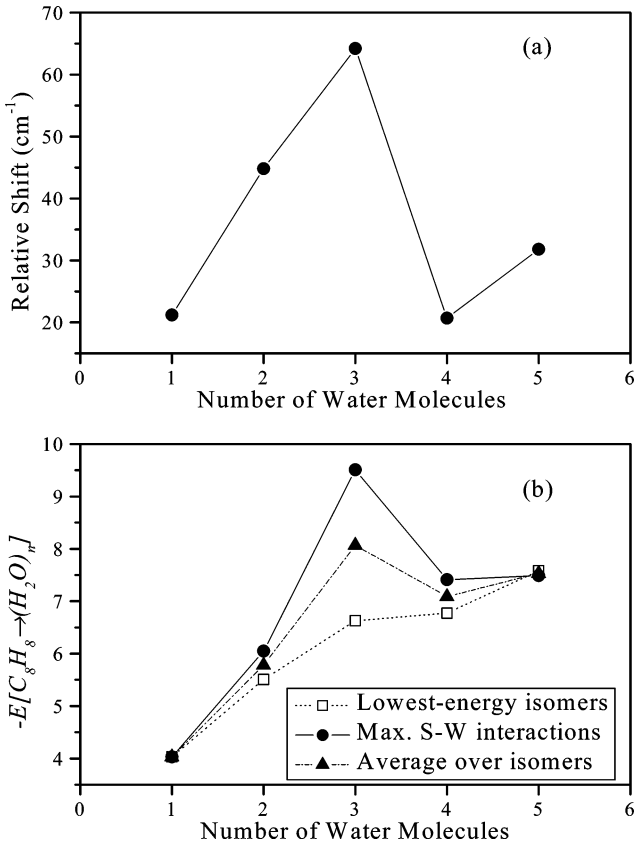

Figure 8. (a) Spectral shifts of the origins of the SW_n clusters, relative to the 0_0^0 band of styrene, as a function of *n*. (b) Calculated interaction energies between styrene and the water subcluster (W_n) in different isomers of the SW_n clusters, as a function of *n*.

IV-4. Reactions within Styrene Cluster Ions. In a previous study, we reported evidence for intracluster reactions following the 248 nm MPI of styrene clusters.[9] These reactions result in a remarkable alternation in the intensity of styrene cations with a strong tendency of the species containing an even number of styrene molecules to form multiple cyclic oligomers during the early steps of propagation.[9] The observed periodicity in the intensity of the styrene ions has been attributed to the formation of indane end groups, which occurs preferentially for the even-numbered ions.

In the present work, we demonstrate that the even/odd alternation in the intensity of styrene cluster ions is also produced following the 193 nm MPI of the styrene clusters as shown in the mass spectrum displayed in Figure 9. The mass spectrum shows an enhanced intensity for the dimer with a strong even/odd alternation in the ion intensities of $(C_8H_8)_n^+$ up to $n = 12$. This is consistent with the formation of indane derivatives during the cationic polymerization of styrene as evident by the isolation of the cyclic styrene dimer 1-methyl-3-phenylindane plus oligomers in the bulk cationic polymerization.[4,40−43] Interestingly, our recent ion mobility study of the gas-phase styrene oligomers confirm the formation of the phenylindane structure following the EI ionization of the styrene clusters.[44] Furthermore, DFT calculations at the

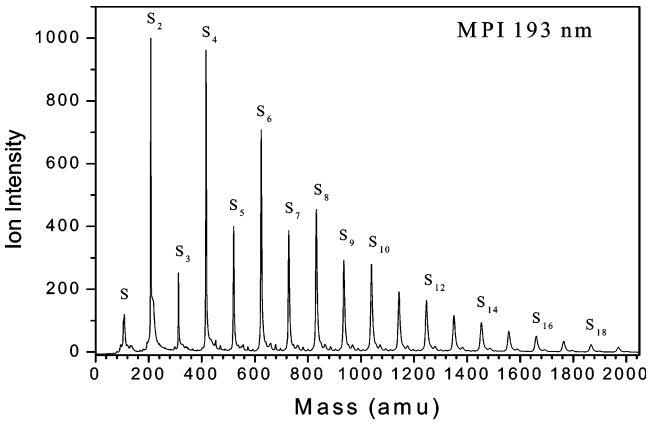

Figure 9. TOF Mass spectrum resulting from the 193 nm MPI of styrene clusters. Note the remarkable even/odd alternation in ion intensity.

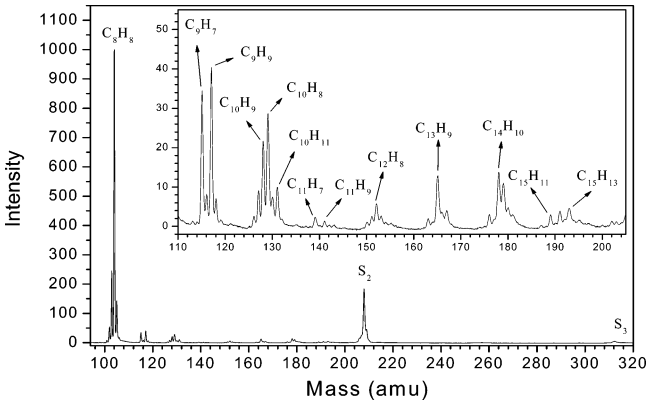

Figure 10. Fragmentation of styrene dimer cation using the 193 nm MPI (20 mJ/pulse).

B3LYP/6-31G** level predicts that the 1-methyl-3-phenylindane cation is more stable than the noncovalent ion−molecule complexes of the styrene dimer cation.[44,45]

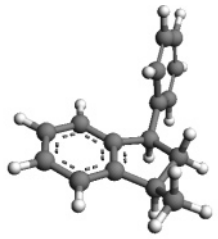

1-methyl-3-phenylindan radical cation

To further support the covalent nature of the styrene dimer ion, we measured the fragments produced following the photodissociation of the styrene dimer ion at 193 nm. The resulting mass spectrum is shown in Figure 10. The observation of the dissociation products $C_{15}H_{13}^+$, $C_{14}H_{10}^+$, $C_{13}H_9^+$, $C_{12}H_8^+$, $C_{10}H_8^+$, $C_{10}H_9^+$, $C_9H_9^+$, and $C_9H_7^+$ corresponding to the loss of the fragments CH_3, C_2H_6, C_3H_7, C_4H_8, C_6H_8, C_6H_7, C_7H_7, and C_7H_9 from the styrene dimer ion confirm the covalent nature of dimer.

The observed dissociation products of the styrene dimer cation are consistent with the formation of 1-methyl-3-phenylindane radical cation. For example, the elimination of the CH_3 group results in the formation of the observed $C_{15}H_{13}$ ion. Also, the subsequent elimination of two hydrogen atoms is consistent with the presence of the CH_2 group in the indane ion. It also appears that the loss of C_2H_4 fragment is followed by elimination of two hydrogen atoms resulting in the formation of the observed

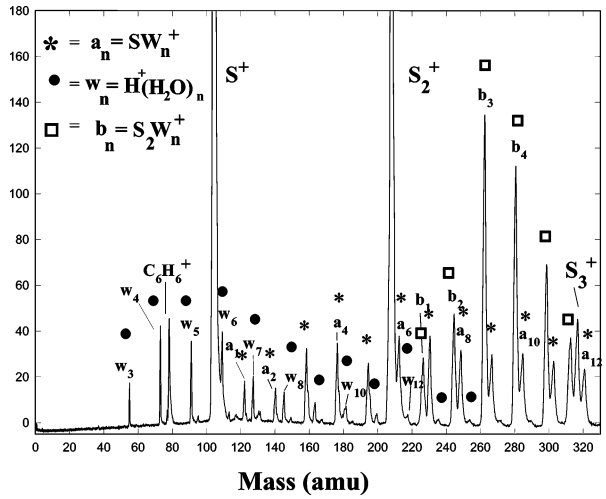

Figure 11. TOF Mass spectrum resulting from the 248 nm MPI of styrene/H_2O binary clusters generated from the expansion of (styrene:water:He) vapor mixture with relative concentrations of $1:(1 \times 10^2):(5 \times 10^7)$, respectively.

$C_{14}H_{10}^+$ ion. The sequential loss of the CH_3 and C_2H_4 fragments results in the generation of the observed $C_{13}H_9^+$ ion. It should be noted that whereas the loss of C_2 and C_3 units is prominent, the eliminations of C_4 and C_5 units are very insignificant. On the other hand, the characteristic eliminations of C_6H_5, C_6H_7 and C_6H_8 indicate the loss of a phenyl group followed by eliminations of H_2 and $H_2 + H$, respectively.

IV-5. Reactions within Styrene (Water)$_n$ Cluster Ions. In this section we investigate the effect of water on the product ions resulting from the MPI of the binary S_mW_n clusters. Following the 248 nm MPI ionization of the binary S_mW_n clusters, protonated water clusters $H^+(H_2O)_n$ are observed starting from $n \geq 3$ as shown in Figure 11. It should be noted that in the absence of styrene, water clusters could not be ionized with the same laser power used to ionize the styrene−water clusters. The H^+W_n clusters could be produced by either dissociative electron transfer (DET, reaction 4) or dissociative proton transfer (DPT, reaction 5), or a combination of both mechanisms.

$$C_8H_8^{\bullet+}(H_2O)_n \rightarrow C_8H_8(H_2O^+)(H_2O)_{n-1} \rightarrow H^+(H_2O)_{n-1} + C_8H_8 + OH \quad (4)$$

$$C_8H_8^{\bullet+}(H_2O)_n \rightarrow H^+(H_2O)_n + C_8H_7^{\bullet} \quad (5)$$

The ET channel is endothermic for small water clusters due to the large difference between the IPs of styrene and water ($\Delta IP = 4.0$ eV).[46] However, for large water clusters reaction 4 may become exothermic as a result of decreasing the IP of $(H_2O)_n$ with n. On the other hand, the calculated PA of the C_8H_7 radical (219 kcal/mol)[47] is nearly similar to the PA of $(H_2O)_3$ (218 kcal/mol), thus indicating that the DPT channel in $C_8H_8^{\bullet+}(H_2O)_n$ becomes exothermic for $n \geq 3$.

The generation of $H^+(H_2O)_n$ with $n \geq 3$ has also been observed following the 248 nm MPI of α-methylstyrene−water clusters. Furthermore, the 248 nm MPI of styrene−methanol clusters results in the generation of protonated methanol clusters $H^+(CH_3OH)_n$ with $n \geq 2$, as shown in Figure 12. In all cases, it appears that solvent molecules (water or methanol) tend to cluster very efficiently around the styrene dimer cation, which appears to be the proton donor in the generation of the protonated water or methanol clusters. This is clearly observed

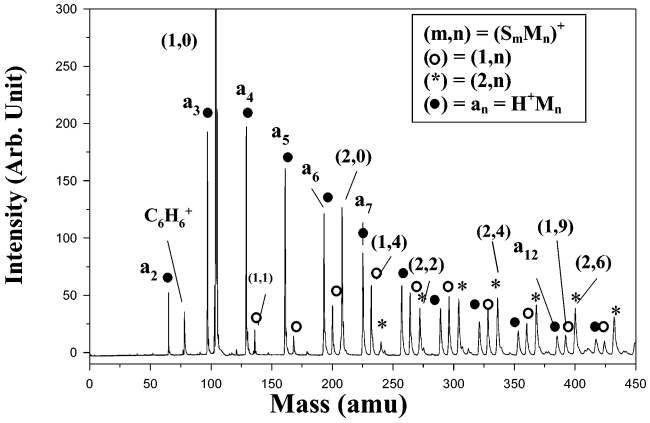

Figure 12. TOF Mass spectrum resulting from the 248 nm MPI of styrene/methanol binary clusters generated from the expansion of (styrene:methanol:He) vapor mixture with relative concentrations of $1:3 \times 10^2:4 \times 10^7$, respectively.

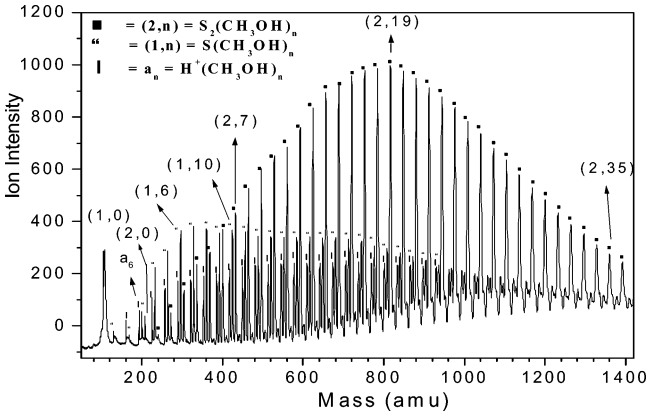

Figure 13. TOF Mass spectrum resulting from the 248 nm MPI of styrene/methanol binary clusters generated from the expansion of (styrene/methanol/He) vapor mixture containing a higher concentration of methanol with relative concentrations of $1:(4 \times 10^4):(7 \times 10^7)$, respectively. Note the extensive addition of methanol clusters on the styrene dimer cation.

in Figure 13, which displays the mass spectrum obtained following the 248 nm MPI of styrene−methanol clusters. The extensive additions of methanol molecules on the styrene dimer cation is intriguing and suggests that the dimer plays a critical role in the proton-transfer (PT) reaction leading to the generation of the protonated methanol clusters. This observation is consistent with our recent study of the R2PI of styrene-(methanol)$_n$ clusters (SM$_n$) where the generation of protonated methanol clusters H$^+$M$_n$ starting at $n \geq 2$ was correlated with the appearance of the $S_2M_n^{\bullet+}$ series suggesting that the PT reaction takes place from styrene dimer cation $C_{16}H_{16}^{\bullet+}$ to the methanol subcluster M$_n$ within the $S_2M_n^{\bullet+}$ clusters.[23]

To verify the unique role of the styrene dimer cation in the PT process, we invetigated the 248 nm MPI of the C_8H_8/D_2O clusters and the resulting mass spectrum is displayed in Figure 14-a. In addition to the $(C_8H_8)^{\bullet+}(D_2O)_n$ and $(C_{16}H_{16})^{\bullet+}(D_2O)_n$ series (labeled Sd$_n$ and S$_2$d$_n$, respectively, in Figure 14), both protonated $H^+(D_2O)_n$ and deuterated $D^+(D_2O)_n$ water clusters (labeled h$_n$ and d$_n$, respectively, in Figure 14) are observed as shown in Figure 14-a. This suggests that both DET and DPT mechanisms are operative within the styrene/water clusters. However, the most interesting result in Figure 14-a is the observation of H/D exchange only within the dimer series $(C_{16}H_{16})^{\bullet+}(D_2O)_n$. All the hydrated ions containing styrene dimer, i.e., $(C_{16}H_{16})^{\bullet+}(D_2O)_n$, including the $C_{16}H_{16}^{\bullet+}$, ion exhibit an additional peak one *m*/*z* unit higher than their nominal *m*/*z*,

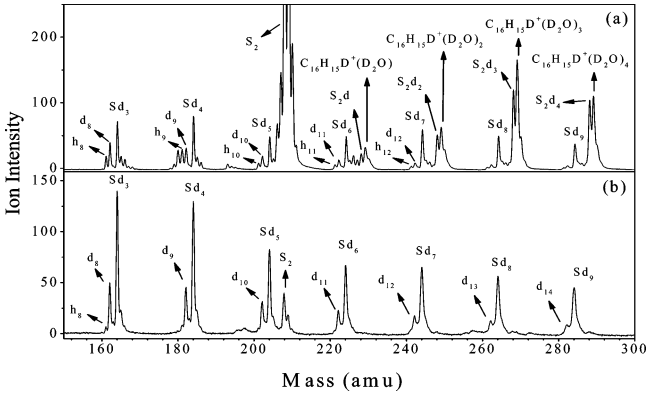

Figure 14. TOF Mass spectra resulting from the 248 nm MPI of styrene/D_2O binary clusters generated from the expansion of (styrene/water/He) vapor mixture with relative concentrations of (a) $1:(1 \times 10^2):(5 \times 10^7)$ and (b) $0.1:(1 \times 10^2):(5 \times 10^7)$. Note the H/D exchange only within the $C_{16}H_{16}^{\bullet+}(D_2O)_n$ series resulting in the obsrvation of the $C_{16}H_{15}D^{\bullet+}(D_2O)_n$ ions in (a).

SCHEME 1

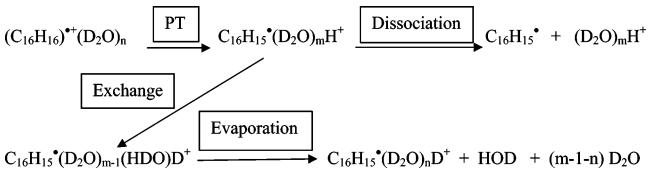

thus confirming the presence of the $C_{16}H_{15}D$ moiety. This means that intracluster PT reactions within $(C_{16}H_{16})^{\bullet+}(D_2O)_m$ clusters produce the $C_{16}H_{15}^{\bullet}(D_2O)_mH^+$ clusters, which are, in effect, $(D_2O)_mH^+$ clusters weakly hydrogen-bonded to a $C_{16}H_{15}^{\bullet}$ radical. Dissociation of these $C_{16}H_{15}^{\bullet}(D_2O)_mH^+$ clusters would produce the observed $H^+(D_2O)_n$ ions (h$_n$ series in Figure 14-a). Also, the $(D_2O)_mH^+$ centers should exchange a hydrogen readily with D_2O molecules within the clusters, leading to $C_{16}H_{15}^{\bullet}(D_2O)_{m-1}$-$(HDO)D^+$ clusters, which upon evaporation of (HDO) produce the observed $C_{16}H_{15}D^{\bullet+}(D_2O)_n$ clusters, one *m*/*z* unit higher than the corresponding $C_{16}H_{16}^{\bullet+}$ $(D_2O)_{m-1}$ ions. The proposed PT-H/D exchange mechanism is outlined in Scheme 1.

To check the validity of the intracluster PT-H/D exchange mechanism, we generated C_8H_8/D_2O clusters using a very small concentration of the styrene vapor in the preexpansion mixture, thus significantly reducing the concentrations of the styrene dimer and higher styrene clusters. The resulting mass spectrum displayed in Figure 14-b shows the presence of the $(C_8H_8)^{\bullet+}$-$(D_2O)_n$ and the DET products $D^+(D_2O)_n$ series (labeled Sd$_n$ and d$_n$, respectively in Figure 14-b). However, the DPT series is completely absent as a result of the absence of the reactive series $(C_{16}H_{16})^{\bullet+}(D_2O)_m$.

Another important result related to the PT-H/D exchange mechanism is the observation of weak metastable peaks in the TOF mass spectrum for all species containing styrene dimer. This effect manifests itself in the broadening of the mass peaks associated with the styrene dimer $[C_{16}H_{15}D^{\bullet+}(D_2O)_n]$, as shown in Figure 14-a. Note that no such broadening is observed in the ions containing the styrene monomer ion [Sd$_n$ series in Figure 14]. The metastable peaks are due to dissociation within the acceleration region of the TOF mass spectrometer. The longer time tail part of the TOF mass peak contains the fragmentation products and the hot ions. If the time scale for the PT, exchange and evaporation steps to generate the $C_{16}H_{15}D^{\bullet+}(D_2O)_n$ ions is nearly the same or shorter than the time of acceleration in the mass spectrometer, metastable peaks will be observed. This may suggest that the PT reaction involves a slow rate probably due

to the existence of an energy barrier. In this case, the slow PT reactions are delayed after the ionization and occur in the acceleration region where they trigger the exchange and evaporation steps that induce the broadening of the associated mass peaks. Alternatively, the PT and the exchange products form rapidly after ionization and then slow evaporations of the HOD molecules take place.

The unique role of the styrene dimer cation in the PT reaction to water clusters is consistent with the structure of the 1-methyl-3-phenylindane proposed for the styrene dimer cation. The presence of a CH_3 group is expected to make the PT process from the 1-methyl-3-phenylindane radical cation energetically more favorable than from the styrene radical cation $C_8H_8^+$. If the resulting $C_{16}H_{15}^{\bullet}$ radical occupies a surface site on the water cluster, then polymerization of further styrene molecules could proceed by a free radical mechanism through the newly generated $C_{16}H_{15}^{\bullet}$ radical.

The observed intracluster proton-transfer reactions are consistent with the detrimental effects of water and methanol on the bulk cationic polymerization of styrene. For example, in radiation-induced polymerization of the bulk monomer free cations are largely responsible for the polymerization under very dry conditions.[4−8] On the other hand, under "wet" conditions where the water concentration $[H_2O] > 10^{-3}$ M, a slower polymerization takes place and is believed to be an entirely free radical process.[6−8] These observations can be fully accounted for by the present results. These results demonstrate that intracluster polymerization is important not only for a fundamental understanding of the initiation mechanisms and the early stages of propagation but also for the elucidation of the effects of inhibitors and retarders on the efficiency of different polymerization channels such as cationic vs free radical mechanisms.

V. Conclusions and Outlook

In the present work, the R2PI spectra, structure, energetic and growth pattern of styrene (water)$_n$ clusters with $n = 1-5$ have been investigated using a combination of experimental and theoretical techniques. The results indicate that the spectral shifts correlate with the interaction energies between styrene and the water subcluster (W_n) within the SW_n clusters. Evidence is presented that points to:

(1) The formation of a stable styrene radical cation dimer following the 193 nm MPI of styrene neutral clusters. Photodissociation of the dimer cation is consistent with the 1-methyl-3-phenylindane structure.

(2) Proton transfer from the styrene dimer cation to the water or methanol subcluster resulting in the formation of protonated water or methanol clusters and a styrene dimer radical that may continue to propagate upon the addition of further styrene molecules via the radical mechanism.

(3) Extensive solvation of the styrene dimer radical within the protonated solvent molecules.

The proton-transfer reactions may explain the strong inhibition effects exerted by small concentrations of water or methanol on the cationic polymerization of styrene. These results provide a molecular level view of the inhibition mechanism exerted by protic solvents on the cationic polymerization of styrene.

Acknowledgment. We gratefully acknowledge financial support from the National Science Foundation Grant # CHE-0414613. We thank W. L. Jorgensen for making his MCLIQ (1990) program available for our use.

References and Notes

(1) Stone, A. D. *The Theory of Intermolecular Forces*; Clarendon: Oxford, 1996.

(2) Tanford, C. *The Hydrophobic Effect: Formation of Micelles and Biological Membranes*; Wiley: New York, 1980.

(3) Kennedy, J. P.; Marechal, E. *Carbocationic Polymerization*; John Wiley & Sons: New York, 1982.

(4) Sawamoto, M.; Kamigaito, M. In *New Methods of Polymer Synthesis*; Ebdon, J. R., Eastmond, G., Eds.; Chapman Hall: London, 1995.

(5) Matyjaszewski, K., Ed. *Cationic Polymerization: Mechanisms, Synthesis, and Applications*; Marcel Dekker: New York, 1996.

(6) Szwarc, M. *Ionic Polymerization Fundamentals*; Hanser: New York, 1996.

(7) Silverman, J.; Tagawa, S.; Kobayashi, H.; Katsumura, Y.; Washio, M.; Tabata, Y. *Radiat. Phys. Chem.* **1983**, *22*, 1039. Gotoh, T.; Yamamoto, M.; Nishijima, Y. *J. Polym. Sci.* **1981**, A-1, *19*, 1047. Machi, S.; Silverman, J.; Metz, D. J. *J. Phys. Chem.* **1972**, *76*, 730. Tagawa, S.; Schnabel, W. *Makromol. Chem. Rapid. Commun.* **1980**, *1*, 345.

(8) Tagawa, S.; Schnabel, W. *Chem. Phys. Lett.* **1980**, *72*, 120.

(9) Pithawalla, Y. B.; Gao, J.; Yu, Z.; El-Shall, M. S. *Macromolecules* **1996**, *29*, 8558.

(10) El-Shall, M. S.; Yu, Z. *J. Am. Chem. Soc*. **1996**, *118*, 13058.

(11) El-Shall, M. S.; Marks, C. *J. Phys. Chem*. **1991**, *95*, 4932.

(12) El-Shall, M. S.; Schriver, K. E. *J. Chem. Phys.* **1991**, *95*, 3001.

(13) Meot-Ner, M.; Sieck, L. W.; El-Shall, M. S.; Daly, G. M. *J. Am. Chem. Soc*. **1995**, *117*, 7737.

(14) El-Shall, M. S.; Daly, G. M.; Yu, Z.; Meot-Ner, M. *J. Am. Chem. Soc*. **1995**, *117*, 7744.

(15) Daly, G. M.; El-Shall, M. S. *J. Phys. Chem.* **1995**, *99*, 5283.

(16) Pithawalla, Y. B.; El-Shall, M. S. In *Solvent-Free Polymerization and Processes*; Hunt, M. O., Long, T. E., Eds.; ACS Symposium Series; American Chemical Society: Washington, DC, 1998; Chapter 15, pp 232−245.

(17) Pithawalla, Y. B.; Gao, J.; El Shall, M. S. In *Polymer Processing in Microgravity*; Pojman, J. A., Ed.; ACS Symposium Series; American Chemical Society: Washington, DC, 2001; Chapter 13, pp 185−202.

(18) Pithawalla, Y. B.; Meot-Ner, M.; Gao, J.; El-Shall, M. S. *J. Phys. Chem. A* **2001**, *105*, 3908.

(19) Ibrahim, Y.; Alsharaeh, E.; Dias, K.; Meot-Ner, M.; El-Shall, M. S. *J. Am. Chem. Soc.* **2004**, *126*, 12766.

(20) Germanenko, I. N.; El-Shall, M. S. *J. Phys. Chem*. **1999**, *103*, 5847.

(21) Daly, G. M.; Wright, D.; El-Shall, M. S. *Chem. Phys. Lett.* **2002**, *331*, 47.

(22) El-Shall, M. S.; Daly, G. M.; Wright, D. *J. Chem. Phys*. **2002**, *116*, 10253.

(23) Mahmoud, H.; Germanenko, I. N.; Ibrahim, Y.; El-Shall, M. S. *J. Phys. Chem. A* **2003**, *107*, 5920−5932.

(24) Jorgensen, W. L.; Chandrasekhar, J.; Madura, J. D.; Impey, R. W.; Klein, M. L. *J. Chem. Phys*. **1983**, *79*, 926.

(25) El-Shall, M. S.; Wright, D.; Ibrahim, Y.; Mahmoud, H. *J. Phys. Chem. A* **2003**, *107*, 5933−5940.

(26) Wright, D.; El-Shall, M. S. *J. Chem. Phys*. **1994**, *100*, 379.

(27) Wright, D.; El-Shall, M. S. *J. Chem. Phys.* **1996**, *105*, 11199.

(28) Jorgensen, W. L.; Severance, D. L. *J. Am. Chem. Soc*. **1990**, *112*, 4768.

(29) Hollas, J. M.; Khalilipour, E.; Thakur, S. N. *J. Mol. Spectrosc*. **1978**, *73*, 240.

(30) Hollas, J. M.; Musa, H.; Ridley, T.; Turner, P. H.; Weisenberger, K. H. *J. Mol. Spectrosc*. **1982**, *94*, 437.

(31) Syage, J. A.; Al Adel, F.; Zewail, A. H. *Chem. Phys. Lett*. **1983**, *103*, 15.

(32) Seeman, J. I.; Grassian, V. H.; Bernstein, E. R. *J. Am. Chem. Soc*. **1988**, *110*, 8542.

(33) Chia, L.; Goodman, L.; Philis, J. G. *J. Chem. Phys*. **1983**, *79*, 593.

(34) Kendler, S.; Haas, Y. *Chem. Phys. Lett*. **1995**, *236*, 324.

(35) Mahmoud, H.; Germanenko, I. N.; Ibrahim, Y.; El-Shall, M. S. *Chem. Phys. Lett*. **2002**, *356*, 91.

(36) Dyke, J. M.; Ozeki, H.; Takahashi, M.; Cockett, M. C. R.; Kimura, K. *J. Chem. Phys*. **1992**, *97*, 8926.

(37) Shalev, E.; Ben-Horin, N.; Jortner, J. *J. Chem. Phys*. **1991**, *94*, 7757.

(38) Easter, D. C.; El-Shall, M. S.; Hahn, M. Y.; Whetten, R. L. *Chem. Phys. Lett.* **1989**, *157*, 277.

(39) Zwier, T. S. *Annu. Rev. Phys. Chem*. **1996**, *47*, 205.

(40) Bertoli, V.; Plesch, P. H. *J. Chem Soc. B* **1968**, 1500.

(41) Gandini, A.; Plesch, P. H. *Eur. Polym*. **1968**, *4*, 55.

(42) Higashimura, T.; Nishii, H. *J. Polym. Sci*. **1977**, *15*, 329.
(43) Sawamoyo, M.; Masuda, T.; Nishii, H.; Higashimura, T. *J. Polym. Sci. Polym. Lett.* **1975**, *13*, 279.
(44) Alsharaeh, E.; Ibrahim, Y.; El-Shall, M. S. *J. Am. Chem. Soc*. **2005**, in press.
(45) Alsharaeh, E. Gas-Phase Studies of Molecular Clusters Containing Metal Cations, and the Ion Mobility of Styrene Oligomers. Ph.D. Dissertation, Virginia Commonwealth University, December 2004.
(46) Linstrom, P. J., Mallard, W. G., Eds. *NIST Chemistry WebBook, NIST Standard Reference Database Number 69*; National Institute of Standards and Technology, Gaithersburg MD, 20899 (http://webbook.nist-.gov), March 2003.
(47) The heat of formation of the styrene radical $C_8H_7^{\bullet}$, $\Delta H_f(C_8H_7^{\bullet})$ was calculated from the NIST database[46] as 83.2 kcal/mol. Using 230.0 kcal/mol as ΔH_f ($C_8H_8^{\bullet+}$), the proton affinity of styrene radical PA($C_8H_7^{\bullet}$) was determined to be 218.9 kcal/mol.